

AN INNOVATIVE APPROACH FOR DETECTION AND CLASSIFICATION OF INTERCARDIAC TUMOR AND THROMBI

K.SHEIK ALI

M.Phil Scholar
Sadakathullah Appa College
Tirunelveli
k.sheikalims@gmail.com

Dr.M.Mohamed Sathik

Principal
Sadakathullah Appa College
Tirunelveli
mmdsadiq@gmail.com

Abstract— The main objective of this project is to propose a new technique for the classification of intracardiac tumor and thrombi in the echocardiograms. The whole method is based on the sparse representation. The mass area in ROI is automatic defined by a coarse-to-fine strategy. A novel globally denoising approach combing the K-SVD and the NLM is employed to eliminate the speckle. The globally despeckling algorithm yields better noise attenuation and edge enhancement, without destroying the important cardiac structures. The K-SVD and a modified ACM with a new external force are applied to segment the mass. The proposed detected contours closely approximate the manually traced ones. Nine features, including the cardiologist's original selected features and new texture characteristics are then extracted. They are capable of distinguishing two masses, whose values are identical with the clinical observations. Finally, all features are implemented to the SRC. The better accuracy and simple implementation make the proposed method beneficial to help the cardiologists make a diagnosis before the surgery

Keywords— *Despeckling, Intracardiac Masses, K-SVD, NLM and Spase Representation*

I. INTRODUCTION

Intracardiac masses are hazardous in cardiovascular disease. Generally, they are abnormal structures within or immediately adjacent to the heart, which must be distinguished for diagnosis. Two main types of intracardiac masses are tumor and thrombus. Primary cardiac tumors are rare entities. Approximately 75% of them in adults are benign, with the majority composed of myxomas. Cardiac tumors may cause obstruction to the left ventricular filling. Patients are present with the embolization intracardiac obstruction and constitutional sighs. Because of the high risk of embolization and sudden death, the tumors need prompt resection. Intracardiac thrombi are seen in a variety of clinical settings and can result in severe morbidity or even death from embolic events. They can occur following myocardial infarction with ventricular thrombus formation, or with a trial fibrillation and mitral stenosis where atrial thrombi predominate. Thrombi in the chambers of the left heart are a

common source of complications like stroke and other arterial embolic syndromes.

Although intracardiac tumors and thrombi are different in pathology, they behave similarly in echocardiography. Often, they are misinterpreted. In most hospitals, echocardiographic identifications are carried out by cardiologists manually. The diagnosis is time-consuming. Recognition depends on the image quality and techniques, as well as the cardiologist's experience. Hence, the demand for an automatic classification is increasing, which is potential to improve the diagnostic accuracy and to guide which case should be recommended for a surgery. The ultrasound image analysis has been successfully employed in the computer-aided diagnosis for cardiovascular disease, such as revealing valuable ultrasound features in early stroke prediction, designing fuzzy rule-based decision support system in the diagnosis of coronary artery, and applying adaptive block matching methodologies in carotid artery wall and plaque dynamics. Nevertheless, it is still challenging in intracardiac masses identification due to the similar echo cardiographic appearances of two masses and the suboptimal image quality including large amount of speckle noise, signal drop-out, artifacts, and missing contours. So a novel method is required to classify the intracardiac tumor and thrombi in echocardiograms.

In most hospitals, echo cardiographic identifications are carried out by cardiologists manually. The diagnosis is time-consuming. Recognition depends on the image quality and techniques, as well as the cardiologist's experience. Hence, the demand for an automatic classification is increasing, which is potential to improve the diagnostic accuracy and to guide which case should be recommended for a surgery. The ultrasound image analysis has been successfully employed in the computer-aided diagnosis for cardiovascular disease, such as revealing valuable ultrasound features in early stroke prediction [7], designing fuzzy rule-based decision support system in the diagnosis of coronary artery [8], and applying adaptive block matching methodologies in carotid artery wall and plaque dynamics [9]. Nevertheless, it is still challenging in intracardiac masses identification due to the similar

echocardiographic appearances of two masses and the suboptimal image quality including large amount of speckle noise, signal drop-out, artifacts, and missing contours. Strzelecki et al. used a neural network to classify and segment different intracardiac masses in tumor echocardiograms in a semiautomatic manner [10]. However, to the best of our knowledge, a fully automatic classification method has not been previously reported in the area of distinguishing intracardiac masses in echocardiograms.

Typically, this kind of classification methods is composed of four parts including despeckling, segmentation, feature extraction, and classification. Unlike the additive, white and Gaussian (AWG) noise, the speckle in the ultrasound image is a multiplicative noise, whose texture often carries useful anatomical information. To achieve the best diagnosis, it is essential to despeckle the images without affecting important image features and destroying anatomical details. Various methods have been used in the ultrasound image despeckling, such as the local statistics [11]–[13], the median filter [14], the speckle reducing anisotropic diffusion (SRAD) [15], [16], and the wavelet-based methods [17]. As locally based methods, they compromise between the averaging (in homogeneous regions) and preserving (at edges and features). These filters are capable of suppressing the speckle, but they remove fine details as well. As for the segmentation, the active contour model (ACM) [18], the level set [19], the active appearance model (AAM) [20], the fuzzy based methods [21], and the graph cut [22] have been evaluated. While these methods may be effective for specific types of images, they are unsatisfactory in the intracardiac mass segmentation owing to the movement of cardiac chamber during the cardiac cycle. In the systolic stage, the chamber shrinks so small that it is filled with an intracardiac mass, with the atrial wall and the mass boundary overlapped. Considerable efforts have been made on the application of the computer aided classification, like the multilayer feedforward artificial neural network (ANN) [10], the back propagation neural network (BPNN) [23], the support vector machine (SVM) [24], and the ensemble learning [25]. Most of these classifiers require training stages and supervision from experienced cardiologists. Therefore, it is meaningful to find a stable classifier with a great capacity of generalization without any training process. In recent years, there has been a growing interest in sparse representation. The sparse concept originated from the transform domain methods, which assumed that true signals could be sparsely represented by a linear combination of few basis elements in the transform domain. Instead of using fixed and orthogonal transforms, images can be described by sparse linear combinations of an over complete dictionary. Applications of the sparse representation include denoising [26], [27], compression [28], regularization in inverse problems [29], [30], and classification [31]. The K-singular value decomposition (KSVD) is one of the typical methods in the sparse representation, which utilizes over complete dictionaries obtained from a preliminary training procedure [26].

This paper compares the performance of three method which are used to convert 2D image into 3D image. The 2D to

3D conversion technique plays a crucial role in the development and promotion of three dimensional television (3DTV) for it can provide adequate supply of high-quality 3D program material. In this paper three methods are analyzed and their performance are compared to find the best method to produce 3D image with high quality. The first method convert 2D image into 3D based on the depth map with edge information. The second method use fusion based depth map information. Finally the third method generate 2D image using random walk algorithm. To analyse the performance of these method several performance metrics are used. This paper uses PSNR,SSIM, MSE and RMSE to analyses the performance. From the experimental results it is shown that the Random Walk method performs better than the other two methods.

The remainder of the paper is organized as follows: In Section II, the overview of proposed method is presented. In Section III, the proposed method is specifically depicted, including its design idea and practical implementation approach. In Section IV, the performance of the proposed method is evaluated. Finally, conclusions are made in Section V.

II. TUMOR OR THROMBI CLASSIFICATION FROM ECHOCARDIOGRAPHIC IMAGES

The overall block diagram of the proposed method is shown in Fig.1. It involves the frame decomposition, automatic region of interests (ROIs) selection, globally despeckling, intracardiac mass segmentation, feature extraction, and classification. The further details of these modules are discussed below:



Fig. 1. Overall Block Diagram of Proposed Methods

III. TUMOR OR THROMBI DETECTION AND CLASSIFICATION PROCEDURE

The proposed method have six modules. They are

1. Frame Decomposition
2. Automatic ROI Selection
3. Global Despeckling
4. Segmentation
5. Feature Extraction
6. Sparse Representation Classification

A. Frame Decomposition:

This is the first module of this project. The cardiologists acquire echocardiogram sequences when diagnosing the disease. To segment the intracardiac mass and evaluate its movement, the echo cardio graphic sequences are divided into consecutive frames beforehand. The typical duration of an echocardiogram sequence is about 3–4 s. The frame rate is 39 frames per second. Each decomposed frame is 480×640 pixels.

Besides the scanned region, an echocardiogram depicts texts and labels, containing information about the patient and scanning transducer. Compared with moving heart in two successive frames, these texts and labels are static. After subtraction of two successive frames, the static information are all removed, while the sector scanned region containing moving heart is remained. Then, the profile of the sector scanned region is detected and a rectangle covering the sector is identified. Finally, the original image is cropped to keep the scanned region for further analysis.

B. Automatic ROI Selection:

After frame decomposition, the next step is to select ROI automatically. In order to focus on the mass area, a ROI containing the mass and its surrounding tissues are defined. A coarse-to-fine iteration strategy for sub windows clustering is applied to automatically select the ROI. The cardiac chamber owns unique texture features, with lower intensities and uniformed distributions. Such intensity differences help to assort the images into two classes: the uniform areas (chamber) and the texture areas (the mass or the myocardium).

The size of the initial sub windows is 40×40 . Each time, several texture features of sub windows, including the mean, the variance, and the gray level co-occurrence matrix (GLCM) [33] are calculated and input into a fuzzy K-means algorithm to cluster the similar sub windows. The uniform sub windows in a coarse position, which, in turn, are searched to get a fine position with half size of sub windows. The iteration ends when all remaining sub windows share the same intensity distribution. In a short axis view echocardiogram, the chamber usually lies near the cardiac center. So in the fine position, the

Euclidian distance between each sub window and the cardiac center is computed to trim off far-away windows and obtain final chamber location. The distance threshold is specified as 80pixels by experienced cardiologists.

C. Global Despeckling

After ROI Selection the next step is to despeckle the global noise. For ultrasound images, the speckle is a Rayleigh-distributed multiplicative noise. It degrades the contrast resolution, limiting the detect ability of small, low-contrast lesions. Different from locally based denoising methods, the NLM extends the “neighborhood” to the “whole image,” taking advantage of the high degree of redundancy in an image. Usually for a fixed configuration, many similar samples can be found in the whole image. With the help of these related patches in far-away areas, rather than the irrelevant ones in local neighborhood, the denoising performance will be greatly improved, especially in the edge preservation. The K-SVD makes the over complete dictionary D containing two kinds of atoms with different sparse coefficients. For the texture area, their coefficients have a small number of non zeros, while the coefficients of the homogeneous areas are all zeros.

D. Segmentation

This is the fourth module of this project. As the basis for the further features extraction, extracting the boundary of the mass is of great importance. Since the intracardiac mass has a base connected with the a trial wall, the mass and the a trial wall should be segmented together. The cardiac chamber and the mass or atrial wall share different intensities. The over complete dictionary D in the K-SVD can discriminate. These two areas by two types of atoms, corresponding to the texture area (intracardiac mass and the a trial wall) and the homogeneous area (cardiac chamber). Here, X_sum is also used to distinguish two areas and convert the original image into a binary one in which the intensities of the homogeneous areas.

After that ACM is applied. The ACM is well-known for image segmentation. It is based on curve evolution and energy function minimization, moving in reaction to two components: the internal forces and the external forces. The internal forces impose constraints on the contour itself, while the external forces push the contour toward image features.

E. Feature Extraction

When identifying intracardiac mass in an echocardiogram sequence, usually the cardiologists make the judgment based on two rules: the motion feature (the mass movement) and the boundary feature (the base length). Although two masses show differences in echo reflections, texture characteristics are visually indistinguishable due to the poor image quality.

They are always omitted clinically. However, texture features, especially the mass internal echo is quite important in the classification. Here, for each segmented mass, three types of features are computed: the motion feature, the boundary feature, and the proposed texture features. The motion feature is a primary factor in mass recognition. During a cardiac cycle, intracardiac tumors show high degree of mobility, while the thrombi stay motionless.

Another essential boundary feature is the base length. An intracardiac tumor has a narrow stalk connected to the a trial wall, whereas a thrombus lies entirely on the wall. The overlap length of these two masses with the a trial wall is different. Here, the base length is the Euclidian distance between two mass-a trial separation points. The base length of a thrombus is much longer than that of a tumor. In addition, texture characteristics derived within the mass are also considered. Three kinds of texture features are extracted. The GLCM is a common method for the texture feature analysis. Five features derived from the GLCM (contrast, entropy, autocorrelation, energy and homogeneity) are computed at $\theta = 0^\circ, 45^\circ, 90^\circ$, and 135° and $d = 1$. The mean intensity inside the mass could also potentially classify the homogenous and inhomogeneous areas. The GLCM features and the mean intensity are the traditional texture descriptors. Furthermore, the mean sparse coefficient is introduced as a new texture feature for a better classification. The sparse coefficients represent the integrative information of the local statistics in a mass. A total of nine features: the mass movement, the base length, five GLCM features, the mean intensity and the mean sparse coefficient are calculated for the further classification.

G. Sparse Representation Classification

A sparse representation-based classifier (SRC) is used to identify an intracardiac mass. It relies on the idea that the test sample can be represented as a linear combination of the training sample. Different from other classifiers, the SRC is a non parametric learning method which does not need a training process but only need the training data.

IV. PERFORMANCE ANALYSIS

A. Expremental Images

A total of 10 clinical echocardiogram sequences were collected at Department of Echocardiography, Arthi Scan Centre, Tirunelveli, Tamilnadu India. They were recorded using the Philips iE33ultrasound imaging system equipped with a S5-1 transducer(imaging bandwidth from 1 to 5 MHz). The sequences were saved in AVI format. The whole classification method was applied on the sequences after they were recorded and stored by the cardiologists. All patients were submitted to surgery. The histopathology of the masses proved that 5 sequences were intracardiac thrombi and 5 were intracardiac tumors.

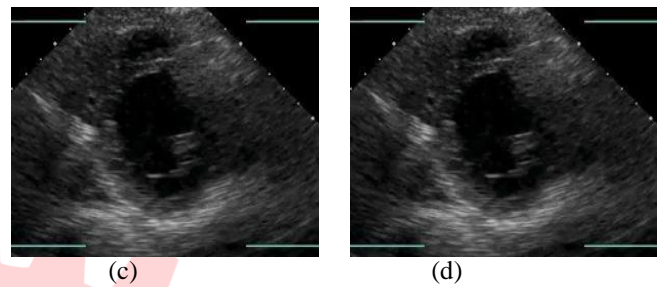
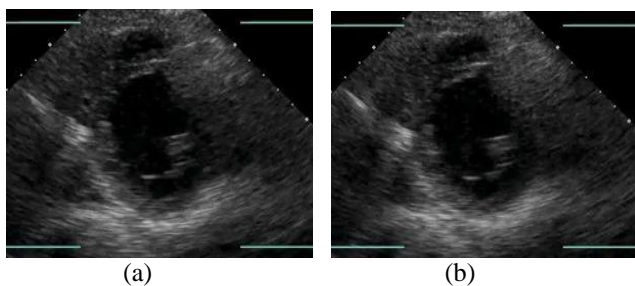


Fig. 4. Expremental Images

B. Performance Analysis

To evaluate the performance of the classify the intracardiac tumor and thrombi techniques several performance metrics are available. This project uses the overall accuracy (ACC), precision rate, the sensitivity (SEN), the specificity (SPE), the positive predicative value (PPV), and the negative predictive value (NPV) to analyses the performance.

Overall Accuracy

Overall Accuracy is the measurement system, which measure the degree of closeness of measurement between the original intracardiac tumor and thrombi and the detected intracardiac tumor and thrombi by the proposed method.

$$ACC = \frac{TP}{TP + FN + FP + TN}$$

Where, TP – True Positive (equivalent with hit)

FN – False Negative (equivalent with miss)

TN – True Negative (equivalent with correct rejection)

FP – False Positive (equivalent with false alarm)

Sensitivity

The sensitivity is the fraction of retrieved instances that are relevant to the find.

$$SEN = \frac{TP}{TP + FN}$$

Where TP = True Positive (Equivalent with Hits)

FN = False Negative (equivalent with miss)

Specificity

The specificity is the fraction of relevant instances that are retrieved according to the query.

$$SPE = \frac{TP}{FP + TN}$$

Where FP = False Positive (equivalent with false alarm)

TN = True Negative (equivalent with correct rejection)

TP – True Positive (equivalent with hit)

Positive Predictive Value

Positive Predictive Value is one of the performance metric which is used to analyse the performance of the classify the intracardiac tumor and thrombi techniques. The PPV can be calculated as,

$$PPV = (1 + \alpha) * \frac{TP}{TP + FP}$$

Where TP – True Positive (equivalent with hit)
FP = False Positive (equivalent with false alarm)

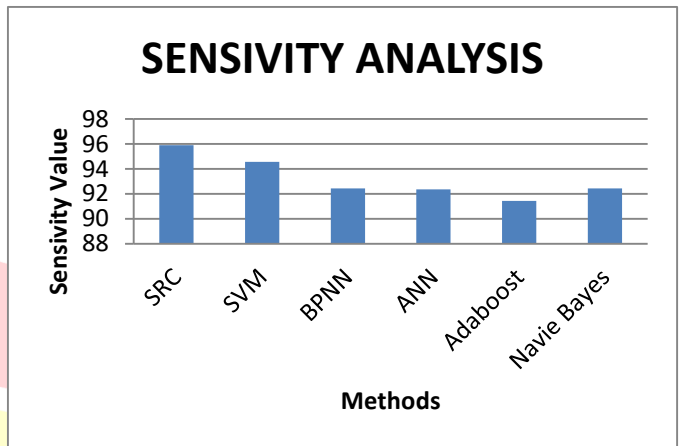
Negative Predictive Value

Negative Predictive Value is one of the performance metric which is used to analyse the performance of the classify the intracardiac tumor and thrombi techniques. The NPV can be calculated as,

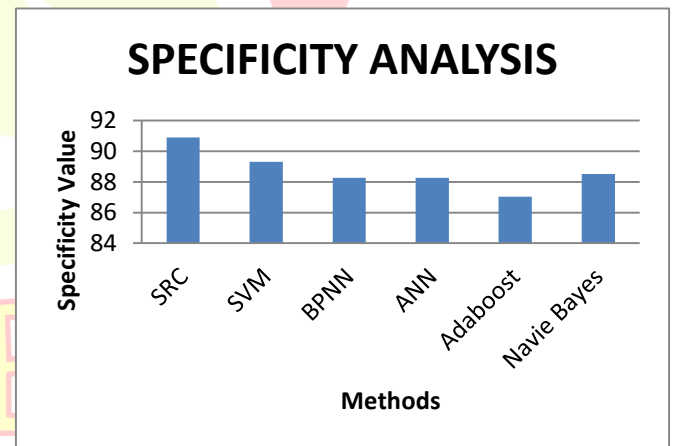
$$NPV = \frac{TN}{TN + FN}$$

Where TN = True Negative (equivalent with correct rejection)
FP = False Positive (equivalent with false alarm)
FN = False Negative (equivalent with miss)

To analysis the performance of the three methods by using the performance metrics which are mentioned above. This is shown in the below tables and graphs

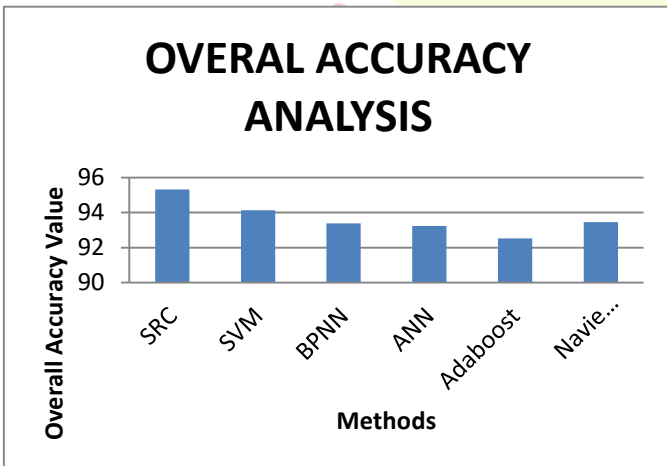


Classification Methods	SPE
SRC	90.9
SVM	89.32
BPNN	88.26
ANN	88.26
Adaboost	87.04
Navie Bayes	88.51

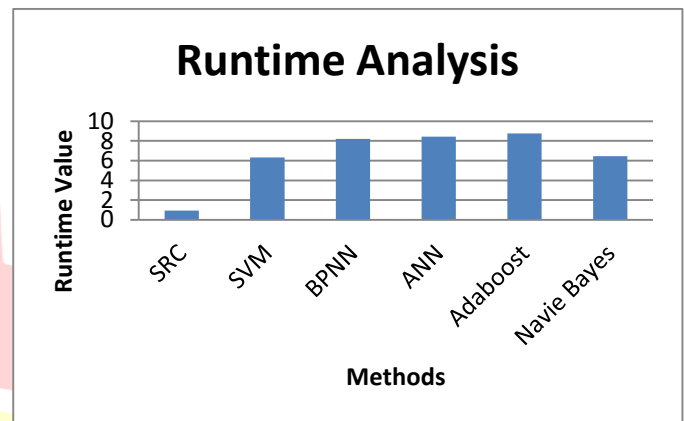
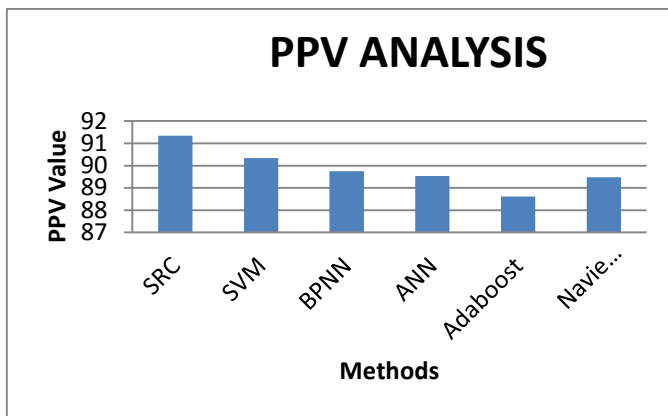


Classification Methods	PPV
SRC	91.35
SVM	90.34
BPNN	89.75
ANN	89.54
Adaboost	88.62
Navie Bayes	89.48

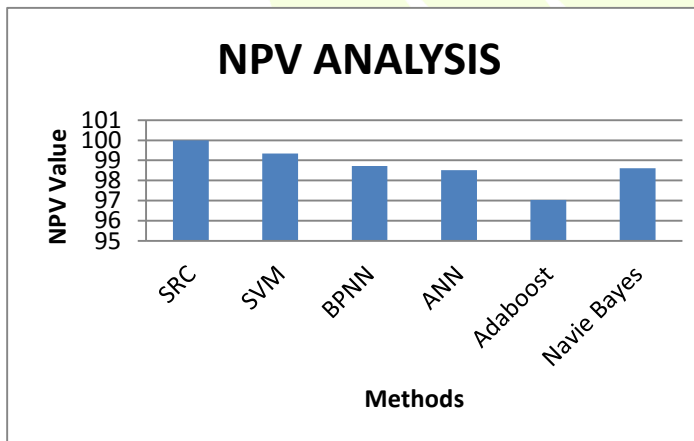
Classification Methods	ACC
SRC	95.32
SVM	94.13
BPNN	93.39
ANN	93.24
Adaboost	92.53
Navie Bayes	93.46



Classification Methods	SEN
SRC	95.91
SVM	94.56
BPNN	92.43
ANN	92.35
Adaboost	91.43
Navie Bayes	92.45



Classification Methods	NPV
SRC	100
SVM	99.34
BPNN	98.72
ANN	98.52
Adaboost	97.04
Navie Bayes	98.61



Classification Methods	Runtime
SRC	0.943
SVM	6.326
BPNN	8.218
ANN	8.432
Adaboost	8.763
Navie Bayes	6.448

V. CONCLUSION

In this project, a new method is proposed for the classification of intracardiac tumor and thrombi in the echocardiograms. The whole method is based on the sparse representation. The massarea in ROI is automatic defined by a coarse-to-fine strategy. A novel globally denoising approach combing the K-SVD and the NLM is employed to eliminate the speckle. The globally despeckling algorithm yields better noise attenuation and edge enhancement, without destroying the important cardiac structures. The K-SVD and a modified ACM with a new external force are applied to segment the mass. The proposed detected contours closely approximate the manually traced ones. Nine features, including the cardiologist's original selected features and new texture characteristics are then extracted. They are capable of distinguishing two masses, whose values are identical with the clinical observations. Finally, all features are implemented to the SRC. The better accuracy and simple implementation make the proposed method beneficial to help the cardiologists make a diagnosis before the surgery.

References

- [1] C. M. Otto, Textbook of Clinical Echocardiography. Philadelphia, PA: Saunders, 2009, pp. 378–398.
- [2] S. Maraj, G. S. Pressman, and V. M. Figueredo, "Primary cardiac tumors," *Int. J. Cardiol.*, vol. 133, no. 2, pp. 152–156, Apr. 2009.
- [3] L. M. Shapiro, "Cardiac tumors: Diagnosis and management," *Heart*, vol. 85, no. 2, pp. 218–222, Feb. 2001.
- [4] M. M. Ragland and Y. Tak, "The role of echocardiography in diagnosing space-occupying lesions of the heart," *J. Clin. Med. Res.*, vol. 4, no. 1, pp. 22–32, Mar. 2006.
- [5] F. Boulay, N. Danchin, J. L. Neimann, J. P. Godenir, and J. P. Houpe, "Echocardiographic features of right atrial thrombi," *J. Clin. Ultrasound*, vol. 14, pp. 601–606, Oct. 1986.
- [6] J. M. Sarjeant, J. Butany, and R. J. Cusimano, "Cancer of the heart: Epidemiology and management of primary tumors and metastases," *Amer. J. Cardiovasc. Drugs*, vol. 3, no. 6, pp. 407–421, 2003.
- [7] S. Golemati, A. Gastouniotti, and K. S. Nikita, "Toward novel noninvasive and low-cost markers for predicting strokes in asymptomatic carotid atherosclerosis: The role of ultrasound image analysis," *IEEE Trans. Biomed. Eng.*, vol. 60, no. 3, pp. 652–658, Mar. 2013.

- [8] M. G. Tsipouras, T. P. Exarchos, D. I. Fotiadis, A. P. Kotsia, K. V. Vakalis, K. K. Naka, and L. K. Michalis, "Automated diagnosis of coronary artery disease based on data mining and fuzzy modeling," *IEEE Trans. Inf. Technol. Biomed.*, vol. 12, no. 4, pp. 447–458, Jul. 2008.
- [9] A. Gastouniotti, S. Golemati, J. S. Stoitsis, and K. S. Nikita, "Carotid artery wall motion analysis from B-mode ultrasound using adaptive block matching: In silico evaluation and in vivo application," *Phys. Med. Biol.*, vol. 58, no. 24, pp. 8647–8661, Nov. 2013.
- [10] M. Strzelecki, A. Materka, J. Drozd, M. Krzeminska-Pakula, and J. D. Kasprzak, "Classification and segmentation of intracardiac masses in cardiac tumor echocardiograms," *Comput. Med. Imaging Graph.*, vol. 30, no. 2, pp. 95–107, Mar. 2006.
- [11] J. S. Lee, "Speckle analysis and smoothing of synthetic aperture radar images," *Comput. Graph Image Process.*, vol. 17, no. 1, pp. 24–32, Sep. 1981.
- [12] V. S. Frost, J. A. Stiles, K. S. Shanmugam, and J. C. Holtzman, "A model for radar images and its application for adaptive digital filtering of multiplicative noise," *IEEE Trans. Pattern Anal. Mach. Intell.*, vol. 4, no. 2, pp. 157–165, Feb. 1982.
- [13] D. T. Kuan, A. A. Sawchuk, T. C. Strand, and P. Chavel, "Adaptive restoration of images with speckle," *IEEE Trans. Acoust. Speech Signal Process.*, vol. 35, no. 3, pp. 373–383, Mar. 1987.
- [14] T. Huang, G. Yang, and G. Tang, "A fast two-dimensional median filtering algorithm," *IEEE Trans. Acoust. Speech Signal Process.*, vol. 27, no. 1, pp. 13–18, Feb. 1979.
- [15] Y. Deng, Y. Wang, and Y. Shen, "Speckle reduction of ultrasound images based on Rayleigh trimmed anisotropic diffusion filter," *Pat. Recognit. Lett.*, vol. 32, no. 13, pp. 1516–1525, Oct. 2011.
- [16] Y. Yu and S. T. Acton, "Speckle reducing anisotropic diffusion," *IEEE Trans. Image Process.*, vol. 11, no. 11, pp. 1260–1270, Nov. 2002.
- [17] S. Gupta, R. C. Chauhan, and S. C. Sexana, "Wavelet-based statistical approach for speckle reduction in medical ultrasound images," *Med. Biol. Eng. Comput.*, vol. 42, no. 2, pp. 189–192, Mar. 2004.
- [18] R. Bellotti, F. Carlo, G. Gargano, S. Tangaro, D. Cascio, E. Catanzariti, P. Cerello, S. C. Cheran, P. Delogu, I. Mitri, C. Fulcheri, D. Grosso, A. Retico, S. Squarcia, E. Tommasi, and B. Golosio, "A CAD system for nodule detection in low-dose lung CTs based on region growing and a new active contour model," *Med. Phys.*, vol. 34, no. 12, pp. 4901–4910, Dec. 2007.
- [19] K. Suzuki, R. Kohlbrenner, M. L. Epstein, A. M. Obajuluwa, J. W. Xu, and M. Hori, "Computer-aided measurement of liver volumes in CT by means of geodesic active contour segmentation coupled with level-set algorithms," *Med. Phys.*, vol. 37, no. 5, pp. 2159–2166, May 2010.
- [20] X. Chen, J. K. Udupa, U. Bagci, Z. Ying, and J. Yao, "Medical image segmentation by combining graph cuts and oriented active appearance models," *IEEE Trans. Image Process.*, vol. 21, no. 4, pp. 2035–2046, Apr. 2012.
- [21] D. Smeets, D. Loeckx, B. Stijnen, B. Dobbelaer, D. Vandermeulen, and P. Suetens, "Semi-automatic level set segmentation of liver tumors combining a spiral-scanning technique with supervised fuzzy pixel classification," *Med. Image Anal.*, vol. 14, no. 1, pp. 13–20, Feb. 2010.
- [22] R. J. Schneider, D. P. Perrin, N. V. Vasilyev, G. R. Marx, P. J. Nido, and R. D. Howe, "Mitral annulus segmentation from 3D ultrasound using graph cuts," *IEEE Trans. Med. Imaging*, vol. 29, no. 9, pp. 1676–1687, Sep. 2010.
- [23] S. Walczak, "Artificial neural network medical decision support tool: Predicting transfusion requirements of ER patients," *IEEE Trans. Inform. Tech. Biomed.*, vol. 9, no. 3, pp. 468–474, Sep. 2005.
- [24] J. Levman, T. Leung, P. Casner, D. Plewes, and A. L. Martel, "Classification of dynamic contrast-enhanced magnetic resonance breast lesions by support vector machines," *IEEE Trans. Med. Imaging*, vol. 27, no. 5, pp. 688–696, May 2008.
- [25] S. Oh, M. S. Lee, and B. Zhang, "Ensemble learning with active example selection for imbalanced biomedical data classification," *IEEE Trans. Comput. Biol. Bioinform.*, vol. 8, no. 2, pp. 316–325, Mar. 2011.
- [26] M. Aharon, M. Elad, and A. Bruckstein, "K-SVD: An algorithm for designing overcomplete dictionaries for sparse representation," *IEEE Trans. Signal Process.*, vol. 54, no. 11, pp. 4311–4322, Nov. 2006.
- [27] K. Dabov, A. Foi, V. Katkovnik, and K. Egiazarian, "Image denoising by sparse 3D transform-domain collaborative filtering," *IEEE Trans. Image Process.*, vol. 16, no. 8, pp. 1–16, Aug. 2007.
- [28] J. Zepeda, C. Guillemot, and E. Kijak, "Image compression using sparse representations and the iteration-tuned and aligned dictionary," *IEEE J. Sel. Topics Signal Process.*, vol. 5, no. 5, pp. 1061–1073, Sep. 2011.
- [29] J. Yang, J. Wright, T. Huang, and Y. Ma, "Image super-resolution via sparse representation," *IEEE Trans. Image Process.*, vol. 19, no. 11, pp. 2861–2873, Nov. 2010.
- [30] S. Malla and G. Yu, "Super-resolution with sparse mixing estimators," *IEEE Trans. Image Process.*, vol. 19, no. 11, pp. 2889–2900, Nov. 2010.
- [31] J. Wright, A. Yang, A. Ganesh, S. S. Sastry, and Y. Ma, "Robust face recognition via sparse representation," *IEEE Trans. Pattern Anal. Mach. Intell.*, vol. 31, no. 2, pp. 210–227, Feb. 2009.
- [32] Y. Guo, Y. Wang, D. Kong, and X. Shu, "Automatic endocardium extraction for echocardiogram," in *Proc. Int. Conf. Biomed. Eng. Inform.*, 2011, pp. 157–161.
- [33] R. Parekh, "Using texture analysis for medical diagnosis," *IEEE Multi-Media*, vol. 19, no. 2, pp. 28–37, Feb. 2012.
- [34] T. C. Aysal and K. E. Barner, "Rayleigh-maximum-likelihood filtering for speckle reduction in ultrasound images," *IEEE Trans. Med. Imaging*, vol. 26, no. 5, pp. 712–727, May 2007.
- [35] A. Buades, B. Coll, and A. Morel, "A review of image denoising algorithms with a new one," *Multiscale Model. Simul.*, vol. 4, no. 2, pp. 490–530, 2005.
- [36] Y. Guo, Y. Wang, and T. Hou, "Speckle filtering of ultrasonic images using a modified non local-based algorithm," *Biomed. Signal Process.*, vol. 6, no. 2, pp. 129–138, Apr. 2011.
- [37] Y. Guo, Y. Wang, D. Kong, and X. Shu, "Automatic segmentation of cardiac tumor in echocardiogram based on sparse representation and modified ACM," in *Proc. Int. Conf. Eng. App. Sci.*, 2012, pp. 22–30.
- [38] M. Kass, A. Within, and D. Terzopoulos, "Snakes: Active contour models," *Int. J. Comput. Vision*, vol. 1, no. 4, pp. 321–331, Jan. 1988.
- [39] C. Xu and J. Prince, "Snake, shapes, and gradient vector flow," *IEEE Trans. Image Process.*, vol. 7, no. 3, pp. 359–369, Mar. 1998.
- [40] L. M. Po and W. C. Ma, "A novel four-step search algorithm for fast block motion estimation," *IEEE Trans. Circuits Syst. Video Technol.*, vol. 6, no. 3, pp. 313–317, Jun. 1996.
- [41] L. Zhang, W. Zhou, P. Chang, J. Liu, Z. Yan, T. Wang, and F. Li, "Kernel sparse representation-based classifier," *IEEE Trans. Signal Process.*, vol. 60, no. 4, pp. 1684–1695, Apr. 2012.
- [42] C. B. Burkhardt, "Speckling in ultrasound B-mode scans," *IEEE Trans. Sonics Ultrason.*, vol. 25, no. 1, pp. 1–6, Jan. 1978.
- [43] C. C. Chang and C. J. Lin, "LIBSVM: A library for support vector machines," *ACM Trans. Intell. Syst. Technol.*, vol. 2, no. 3, pp. 1–27, Apr. 2011.